

*Full Length Research Paper*

# Visco-elastic MHD flow of Walters liquid B fluid and heat transfer over a non-isothermal stretching sheet

Esmail Ghasemi, Mahmoud Bayat\* and Mahdi Bayat

Department of Civil Engineering, Shirvan Branch, Islamic Azad University, Shirvan, Iran.

Accepted 06 July, 2011

**An analytic study has been carried on steady MHD flow and heat transfer in a visco-elastic fluid flow over a semi-infinite, impermeable and non-isothermal stretching sheet with internal heat generation/absorption in the presence of radiation. Thermal conductivity is assumed to vary linearly with temperature. The governing partial differential equations are converted into ordinary differential equations by a similarity transformation. These equations are solved by homotopy analysis method (HAM). The results are then compared with numerical ones which showed excellent agreement. The temperature profiles are shown graphically for different physical parameters.**

**Key words:** Walters liquid B, stretching sheet, visco-elastic fluid, heat transfer, magneto hydrodynamics, HAM.

## INTRODUCTION

Boundary layer flow over a stretching sheet has gained much interest in recent years because of its numerous industrial applications in the polymer processing of a chemical engineering plant and in metallurgy for the metal processing. Crane (1970) was first to formulate this problem to study a steady two-dimensional boundary layer flow caused by stretching of a sheet that moves in its plane with a velocity which varies linearly with the distance from a fixed point on the sheet. Many investigators have extended the work of Crane (1970) to study heat and mass transfer under different physical situations by including quadratic and higher order stretching velocity (Gupta et al., 1977; Chen and Char, 1988; Datta et al., 1985; McLeod et al., 1987; Chiam, 1988, 1996). All these works are restricted to Newtonian fluid flows which have received much attention in the last three decades due to their occurrence in nature and their increasing importance in industry. Different types of non-Newtonian fluids are visco-elastic fluid, couple stress fluid, micro polar fluid and power-law fluid. Rajagopal et al. (1984) and Siddappa and Abel (1985) studied the flow of a visco-elastic fluid flow over a stretching sheet. Troy et al. (1987), Wen-Dong (1989), Sam Lawrence and Rao

(1985) and McLeod and Rajagopal (1987) have discussed the problem of uniqueness and non-uniqueness of the flow of a non-Newtonian visco-elastic fluid over a stretching sheet. Abel and Veena (1988) studied the heat transfer of a visco-elastic fluid over a stretching sheet. Bujurke et al. (1987) have investigated the heat transfer phenomena in a second order fluid flow over a stretching sheet with internal heat generation and viscous dissipation. Prasad et al. (2000) analyzed the problem of a visco-elastic fluid flow and heat transfer in a porous medium over a non-isothermal stretching sheet with variable thermal conductivity. Prasad et al. (2003) have investigated on the diffusion of a chemically reactive species of a non-Newtonian fluid immersed in a porous medium over a stretching sheet. In recent years, the study of MHD flow and heat transfer problems has gained considerable interest because of its extensive engineering applications and may find its applications in polymer technology related to the stretching of plastic sheets. Also, many metallurgical processes involve the cooling of continuous strips or filaments by drawing them through a quiescent fluid and while drawing these strips, they are sometimes stretched. The rate of cooling can be controlled by drawing such strips in an electrically conducting fluid subjected to a magnetic field in order to get the final products of desired characteristics as the final product greatly depend on the rate of cooling. In view of this, the study of MHD flow of Newtonian and

---

\*Corresponding author. E-mail: [mbayat14@yahoo.com](mailto:mbayat14@yahoo.com). Tel: +98 111 3234205.

non-Newtonian flow over a stretching sheet was carried out by many researchers (Sarpakaya, 1961; Pavlov, 1974; Chakrabarti and Gupta, 1979; Char, 1994; Andersson, 1992; Datti, 2004; Liao, 2003; Xu H et al., 2005). In the present paper, we study the effect of variable thermal conductivity on the heat transfer of a non-Newtonian visco-elastic fluid of the type Walters Liquid B, where thermal conductivity is a function of temperature, subjected to a magnetic field, over a non-isothermal stretching sheet with internal heat generation / absorption. We have assumed that the thermal conductivity is a linear function of the temperature. Further, we consider two cases of non-isothermal boundary conditions namely:

1. Surface with prescribed surface temperature (PST Case) and
2. Surface with prescribed wall heat flux (PHF Case).

The momentum and energy equations are highly non-linear and coupled form of partial differential equations (PDEs). These PDEs are then converted to couple non-linear ordinary differential equations (ODEs) by using the similarity variables along with the appropriate boundary conditions. In this paper, we propose to solve these ordinary differential equations analytically by homotopy analysis method (Moghimi et al., 2010; Bararnia et al., 2010; Liao, 2003). Computations are carried out for temperature profiles, Nusselt number when the walls are maintained with prescribed surface temperature and prescribed wall heat flux. Emphasis is given to the effect of thermal radiation on the other physical characteristics.

**BASIC IDEA OF HAM**

Let us assume the following non-linear differential equation in form of:

$$N[u(\tau)] = 0, \tag{1}$$

where N is a non-linear operator,  $\tau$  is an independent variable and  $u(\tau)$  is the solution of the equation. We define the function,  $\phi(\tau, p)$  as follows:

$$\lim_{p \rightarrow 0} \phi(\tau, p) = u_0(\tau), \tag{2}$$

where,  $p \in [0,1]$  and  $u_0(\tau)$  is the initial guess which satisfies the initial or boundary conditions and

$$\lim_{p \rightarrow 1} \phi(\tau, p) = u(\tau), \tag{3}$$

And by using the generalized homotopy method, Liao's so-called zero-order deformation Equation 1 will be:

$$(1 - p)L[\phi(\tau, p) - u_0(\tau)] = p\hbar H(\tau)N[\phi(\tau, p)], \tag{4}$$

where  $\hbar$  is the auxiliary parameter which helps us increase the results convergence,  $H(\tau)$  is the auxiliary function and  $L$  is the linear operator. It should be noted that there is a great freedom to choose the auxiliary parameter  $\hbar$ , the auxiliary function  $H(\tau)$ , the initial guess  $u_0(\tau)$  and the auxiliary linear operator  $L$ . This freedom plays an important role in establishing the keystone of validity and flexibility of HAM as shown in this paper. Thus, when  $p$  increases from 0 to 1 the solution  $\phi(\tau, p)$  changes between the initial guess  $u_0(\tau)$  and the solution  $u(\tau)$ . The Taylor series expansion of  $\phi(\tau, p)$  with respect to  $p$  is:

$$\phi(\tau, p) = u_0(\tau) + \sum_{m=1}^{+\infty} u_m(\tau)p^m \tag{5}$$

And

$$u_0^{[m]}(\tau) = \left. \frac{\partial^m \phi(\tau, p)}{\partial p^m} \right|_{p=0}, \tag{6}$$

where  $u_0^{[m]}(\tau)$  for brevity is called the  $m$ th order of deformation derivation which reads:

$$u_m(\tau) = \frac{u_0^{[m]}(\tau)}{m!} = \frac{1}{m!} \left. \frac{\partial^m \phi(\tau, p)}{\partial p^m} \right|_{p=0}, \tag{7}$$

It is clear that if the auxiliary parameter  $\hbar = -1$  and auxiliary function  $H(\tau) = 1$ , then Equation 1 will become:

$$(1 - p)L[\phi(\tau, p) - u_0(\tau)] + p(\tau)N[\phi(\tau, p)] = 0, \tag{8}$$

This statement is commonly used in HPM procedure. Indeed, in HPM we solve the non-linear differential equation by separating any Taylor expansion term. Now we define the vector of:

$$\vec{u}_m = \{\vec{u}_1, \vec{u}_2, \vec{u}_3, \dots, \vec{u}_n\} \tag{9}$$

According to the definition in Equation 7, the governing equation and the corresponding initial conditions of  $u_m(\tau)$  can be deduced from zero-order deformation Equation 1. Differentiating Equation 1  $m$  times with respect to the embedding parameter  $p$  and setting  $p = 0$  and finally dividing by  $m!$ , we will have the so-called  $m$ th-order deformation equation in the form:

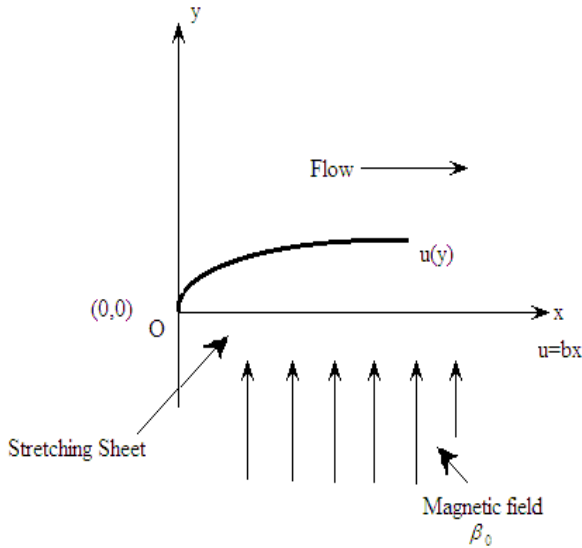


Figure 1. Physical model for hydromagnetic stretching sheet flow.

$$L[u_m(\tau) - \chi_m u_{m-1}(\tau)] = \hbar H(\tau) R(\bar{u}_{m-1}), \tag{10}$$

where

$$R_m(\bar{u}_{m-1}) = \frac{1}{(m-1)!} \left. \frac{\partial^{m-1} N[\phi(\tau, p)]}{\partial p^{m-1}} \right|_{p=0}, \tag{11}$$

and

$$\chi_m = \begin{cases} 0 & m \leq 1 \\ 1 & m > 1 \end{cases}, \tag{12}$$

So by applying inverse linear operator to both sides of the linear equation, Equation 1, we can easily solve the equation and compute the generation constant by applying the initial or boundary condition.

### GOVERNING EQUATIONS AND SIMILARITY ANALYSIS

#### Flow analysis

Consider a steady, laminar flow of an incompressible and electrically conducting visco-elastic fluid over a semi-infinite, impermeable stretching sheet (Figure 1). Two equal and opposite forces are introduced along the x-axis so that the sheet is stretched with a speed proportional to the distance from the origin. The resulting motion of the otherwise quiescent fluid is thus caused solely by the moving surface. A uniform magnetic field of strength  $B_0$

is imposed along y-axis. This flow satisfies the rheological equation of state derived (Beard et al., 1964). The steady two dimensional boundary layer equations for this flow in usual notation are

$$\frac{\partial u}{\partial x} + \frac{\partial v}{\partial y} = 0, \tag{13}$$

$$u \frac{\partial u}{\partial x} + v \frac{\partial u}{\partial y} = \gamma \frac{\partial^2 u}{\partial y^2} - \frac{\sigma B_0^2}{\rho} u - k_0 \left\{ u \frac{\partial^3 u}{\partial x \partial y^2} + v \frac{\partial^3 u}{\partial y^3} + \frac{\partial u \partial^2 u}{\partial x \partial y^2} - \frac{\partial u \partial^2 u}{\partial y \partial x y} \right\}, \tag{14}$$

In deriving these equations it is assumed, in addition to the usual boundary layer approximations that the contribution due to the normal stress is of the same order of magnitude as the shear stress. Here, it is assumed that the magnetic field is applied in the transverse direction of the sheet and the induced magnetic field is negligible. The boundary conditions applicable to the flow problem are

$$\begin{aligned} u(x,0) &= bx, \quad v(x,0) = 0, \\ u(x,y) &\rightarrow 0 \quad \text{as } y \rightarrow \infty, \\ u_y(x,y) &\rightarrow 0 \quad \text{as } y \rightarrow \infty, \end{aligned} \tag{15}$$

with  $b > 0$ . Here  $x$  and  $y$  are, respectively, the directions along and perpendicular to the sheet,  $u$  and  $v$  are the velocity components along  $x$  and  $y$  directions.  $\rho$ ,  $\gamma$ ,  $B_0$ ,  $\sigma$  and  $k_0$  are, respectively, the density, kinematic viscosity, applied magnetic field, induced magnetic field and coefficient of visco-elasticity. The flow is caused solely by the stretching of the sheet, the free stream velocity being zero. Equations 13 and 14 admit a self-similar solution of the form that follows:

$$u = bx f_\eta(\eta), \quad v = -\sqrt{b\gamma} f(\eta), \quad \eta = \sqrt{\frac{b}{\gamma}} y \tag{16}$$

where subscript  $\eta$  denotes the differentiation with respect to  $\eta$ . Clearly  $u$  and  $v$  satisfy Equation 13 identically. Substituting these new variables in Equation 14, we have:

$$f'^2 - ff'' - f''' + M_n f' + k_1 \{ 2ff''' - ff^{iv} - f''^2 \} = 0, \tag{17}$$

where  $M_n = \frac{\sigma B_0^2}{\rho b}$  is the magnetic parameter,

$k_1 = \frac{k_0 b}{\gamma}$  is the visco-elastic parameter,

and prime denotes derivatives with respect to  $\eta$ . Using Equation 16, the boundary conditions become:

$$f(\eta) = 0 \quad \text{at} \quad \eta = 0, \tag{18a}$$

$$f'(\eta) = 1 \quad \text{at} \quad \eta = 0, \tag{18b}$$

$$f'(\eta) \rightarrow 0 \quad \text{at} \quad \eta \rightarrow \infty, \tag{18c}$$

It is interesting to note that the Equation 17 has exact analytical solution of the form

$$f' = e^{-\alpha\eta}, \quad \alpha > 0 \tag{19}$$

Satisfying the boundary conditions Equation 18. Integration of Equation 18 and using of it, gives:

$$f = \frac{1}{\alpha}(1 - e^{-\alpha\eta}), \quad \text{where} \quad \alpha = \sqrt{\frac{(1 + M_n)}{(1 - k_1)}} \tag{20}$$

Therefore the velocity components are give as:

$$u = bxe^{-\alpha\eta}, v = -\sqrt{b\gamma} \frac{1 - e^{-\alpha\eta}}{\alpha} \tag{21}$$

### Heat transfer analysis

The energy equation for a fluid with variable thermal conductivity in the presence of internal heat generation/absorption for the two-dimensional flow is given (Chiam, 1977):

$$\rho C_p \left( u \frac{\partial T}{\partial x} + v \frac{\partial T}{\partial y} \right) = k(T) \frac{\partial^2 T}{\partial y^2} + \frac{\partial k(T)}{\partial y} \frac{\partial T}{\partial y} + \dot{q}(T - T_\infty) - \frac{\partial q_r}{\partial y}, \tag{22}$$

Where  $C_p$  is the specific heat at constant pressure,  $T$  is the temperature of the fluid,  $T_\infty$  is the constant temperature of the fluid far away from the sheet,  $k(T)$  is the temperature-dependent thermal conductivity and  $\dot{q}$  is the volumetric rate of heat generation. We consider the temperature-thermal conductivity relationship of the following form (Chiam, 1977):

$$k(T) = k_\infty \left( 1 + \frac{\epsilon}{\Delta T} (T - T_\infty) \right), \tag{23}$$

where  $\Delta T = T_w - T_\infty$ ,  $T_w$  is the sheet temperature,  $\epsilon = -\frac{k_w - k_\infty}{k_\infty}$  is a small parameter and  $k_\infty$  is the

conductivity of the fluid far away from the sheet. By using Rosseland approximation (Quinn, 1992), the radiative heat flux is given by:

$$q_r = -\frac{4\sigma^*}{3k^*} \frac{\partial T^4}{\partial y}, \tag{24}$$

where  $\sigma^*$  and  $k^*$  are, respectively, the Stephan–Boltzmann constant and the mean absorption coefficient. We assume that the differences within the flow are such that  $T^4$  can be expressed as a linear function of temperature. This is accomplished by expanding  $T^4$  in a Taylor series about  $T_\infty$  and neglecting higher order terms, thus:

$$T^4 \cong 4T_\infty^3 T - 3T_\infty^4 \Rightarrow q_r = -\frac{16\sigma^* T_\infty^3}{3k^*} \frac{\partial T}{\partial y}, \tag{25}$$

Substituting Equations 25 and 23 in Equation 22, we have:

$$\rho C_p \left( u \frac{\partial T}{\partial x} + v \frac{\partial T}{\partial y} \right) = k_\infty \left( 1 + \frac{\epsilon}{\Delta T} (T - T_\infty) \right) \frac{\partial^2 T}{\partial y^2} + k_\infty \frac{\epsilon}{\Delta T} \left( \frac{\partial T}{\partial y} \right)^2 + \dot{q}(T - T_\infty) + \frac{16\sigma^* T_\infty^3}{3k^*} \frac{\partial^2 T}{\partial y^2}, \tag{26}$$

The thermal boundary conditions depend on the type of heating process under consideration. Here, we consider two different heating processes, namely, (1) prescribed surface temperature and (2) prescribed wall heat flux, varying with the distance. The boundary conditions assumed for solving Equation (26) are given as:

$$\left. \begin{aligned} T = T_w = T_\infty + A \left( \frac{x}{l} \right)^r \quad (PST \text{ Case}) \\ -k \frac{\partial T}{\partial y} = q_w = D \left( \frac{x}{l} \right)^r \quad (PHF \text{ Case}) \end{aligned} \right\} \text{at } y=0 \text{ and}, \tag{27}$$

$$T \rightarrow T_\infty \quad \text{as} \quad y \rightarrow \infty, \tag{28}$$

where  $A$  is a constant and depends on the thermal properties of the liquid,  $r$  is the wall temperature parameter,  $q_w$  is the heat flux on the wall surface,

$l = \sqrt{\frac{\gamma}{b}}$  is chosen as characteristic length and  $D$  is a constant. It is obvious now that

$$\Delta T = T_w - T_\infty = \begin{cases} A \left( \frac{x}{l} \right)^r & PST \text{ Case} \\ \frac{D}{k_\infty} \left( \frac{x}{l} \right)^r \sqrt{\frac{\gamma}{b}} & PHF \text{ Case} \end{cases} \tag{29}$$

We now use a dimensionless scaled  $\eta$ -dependent temperature of the form

$$\theta(\eta) = \frac{T - T_\infty}{\Delta T}, \tag{30}$$

The imminent advantage of using Equation 27 is that the temperature-dependent thermal conductivity turns out to be  $x$ -independent. Equation 26 reduces to the non-linear differential equation using Equations 16, 29 and 30:

$$(1 + \epsilon\theta + Nr)\theta'' + Pr(f\theta' - (rf' - \beta)\theta) + \epsilon\theta'^2 = 0, \tag{31}$$

where,  $Pr = \left(\frac{\mu C_p}{k_\infty}\right)$ , is the Prandtl number,

$Nr = \frac{16\sigma^* T_\infty^3}{3k^* k_\infty}$  is the radiation parameter and

$\beta = \frac{\dot{q}}{\rho C_p b}$  is the heat source/sink parameter.

Equations 27 and 28 on using Equations 29 and 30 can be written as:

$$\left. \begin{aligned} \theta(0) &= 1 && (PST \text{ Case}) \\ \theta'(0) &= -1 && (PHF \text{ Case}) \end{aligned} \right\}, \quad \theta(\infty) = 0, \tag{32}$$

**ANALYTIC SERIES SOLUTIONS USING HOMOTOPY ANALYSIS METHOD**

In general, it is quite difficult to solve highly non-linear partial differential equations analytically. The much celebrated perturbation technique can be used for this purpose but only for weakly non-linear problems. Liao (1992a, 1992b) developed a new analytical technique called the homotopy analysis method (HAM) to tackle such non-linear problems (Liao, 1992, 1997, 1999, 2003). Being different from perturbation technique, HAM does not need any small parameter. As a matter of fact, the homotopy analysis method can be regarded as a unification of previous non-perturbation techniques such as Adomian method. By its very nature, HAM provides a family of series solutions whose convergence region can be adjusted and controlled by an auxiliary parameter. It is worth mentioning that the homotopy analysis method has successfully been applied to many non-linear problems in solid and fluid mechanics (Liao, 1999, 2002).

The first step in the HAM is to find a set of base functions to express the sought solution of the problem under investigation. As mentioned by Liao (Liao, 2002), a solution may be expressed with different base functions, among which some converge to the exact solution of the problem faster than others. Noting that, from the boundary conditions of Equations 18 and 20 and according to rule of solution expression, it is straightforward to choose the initial guesses for  $f(\eta)$  and  $\theta(\eta)$  in the following forms:

$$f_0(\eta) = 1 - \exp(-\eta), \tag{33}$$

$$\theta_0(\eta) = \exp(-\eta), \quad \text{for PST Case} \tag{34a}$$

$$\theta_0(\eta) = \exp(-\eta), \quad \text{for PHF Case} \tag{34b}$$

Furthermore, we choose

$$L_1[f] = f''' - f', \tag{35}$$

$$L_2[\theta] = \theta'' + \theta', \tag{36}$$

As our auxiliary linear operators, which have the following properties:

$$L_1(c_3 \exp(-\eta) + c_2 \eta + c_1) = 0, \tag{37}$$

$$L_2(c_4 \exp(-\eta) + c_5) = 0, \tag{38}$$

And  $c_i (i = 1 - 5)$  are integral constants. Then we construct the so-called *Zeroth-order deformation equations*:

$$(1 - p)L_1[f(\eta, p) - f_0(\eta)] = p\hbar_1 N_1[f(\eta, p)], \tag{39}$$

$$(1 - p)L_2[\theta(\eta, p) - \theta_0(\eta)] = p\hbar_2 N_2[f(\eta, p), \theta(\eta, p)], \tag{40}$$

subject to the boundary conditions that follows:

$$f(0, p) = 0, f'(0, p) = 1, f'(\infty, p) = 0, \tag{41}$$

$$\theta(\infty, p) = 0, \left\{ \begin{aligned} \theta(0, p) &= 1 && \text{for PST Case,} \\ \theta'(0, p) &= -1 && \text{for PHF Case} \end{aligned} \right. \tag{42}$$

Under the definitions

$$\begin{aligned} N_1[f(\eta, p)] &= \left(\frac{\partial f(\eta, p)}{\partial \eta}\right)^2 - f(\eta, p) \frac{\partial^2 f(\eta, p)}{\partial \eta^2} - \frac{\partial^3 f(\eta, p)}{\partial \eta^3} + M_n \frac{\partial f(\eta, p)}{\partial \eta} \\ &+ k_1 \left\{ 2 \frac{\partial f(\eta, p)}{\partial \eta} \frac{\partial^3 f(\eta, p)}{\partial \eta^3} - f(\eta, p) \frac{\partial^4 f(\eta, p)}{\partial \eta^4} - \left(\frac{\partial^2 f(\eta, p)}{\partial \eta^2}\right)^2 \right\}, \end{aligned} \tag{43}$$

$$\begin{aligned} N_2[f(\eta, p), \theta(\eta, p)] &= (1 + \epsilon\theta(\eta, p) + Nr) \frac{\partial^2 \theta(\eta, p)}{\partial \theta^2} \\ &+ Pr \left( f(\eta, p) \frac{\partial \theta(\eta, p)}{\partial \theta} - \left( r \frac{\partial f(\eta, p)}{\partial \eta} - \beta \right) \theta \right) + \epsilon \left( \frac{\partial \theta(\eta, p)}{\partial \theta} \right)^2, \end{aligned} \tag{44}$$

where  $P \in [0,1]$  denotes the embedding parameter,  $\hbar_1$  and  $\hbar_2$  indicates non-zero auxiliary parameters. Obviously, for  $p = 0$  and  $p = 1$ , we have:

$$f(\eta,0) = f_0(\eta), \theta(\eta,0) = \theta_0(\eta), \tag{45}$$

$$f(\eta,1) = f(\eta), \theta(\eta,1) = \theta(\eta), \tag{46}$$

By Taylor's power series and using Equations 48 and 49,  $f(\eta; p)$  and  $\theta(\eta; p)$  can be expanded in a power series of  $p$  as follows:

$$f(\eta, p) = f(\eta,0) + \sum_{m=1}^{+\infty} f_m(\eta) p^m, \tag{47}$$

$$\theta(\eta, p) = \theta(\eta,0) + \sum_{m=1}^{+\infty} \theta_m(\eta) p^m, \tag{48}$$

Where

$$f_m(\eta) = \left. \frac{1}{m!} \frac{\partial^m f(\eta, p)}{\partial p^m} \right|_{p=0}, \tag{49}$$

$$\theta_m(\eta) = \left. \frac{1}{m!} \frac{\partial^m \theta(\eta, p)}{\partial p^m} \right|_{p=0}, \tag{50}$$

Note that the convergence regions of the series Equations 48 and 49 are dependent upon the auxiliary parameters  $\hbar_1$  and  $\hbar_2$ . If these auxiliary parameters are properly chosen so that series Equations 48 and 49 are convergent at  $p = 1$ , therefore using Equations 46 and 47 we have:

$$f(\eta) = f_0(\eta) + \sum_{m=1}^{+\infty} f_m(\eta) p^m, \tag{51}$$

$$\theta(\eta) = \theta_0(\eta) + \sum_{m=1}^{+\infty} \theta_m(\eta) p^m, \tag{52}$$

Differentiating the Equations 40 and 41  $m$  times with respect to  $p$  and then setting  $p = 0$  and finally dividing them by  $m!$  we obtain the so-called  $m$ th-order deformation equations for  $f_m(\eta)$  and  $\theta_m(\eta)$  (Liao, 2007) as:

$$L_1[f_m(\eta) - \chi_m f_{m-1}(\eta)] = \hbar_1 R_m^f, \tag{53}$$

$$L_2[\theta_m(\eta) - \chi_m \theta_{m-1}(\eta)] = \hbar_2 R_m^\theta, \tag{54}$$

subject to the boundary conditions given as:

$$f_m(0) = 0, f'_m(0) = 0, f'_m(\infty) = 0, \tag{55}$$

$$\theta_m(\infty) = 0, \begin{cases} \theta_m(0) = 0 & \text{for PST Case,} \\ \theta'_m(0) = 0 & \text{for PHF Case} \end{cases} \tag{56}$$

under the definitions we have:

$$f_m(0) = 0, f'_m(0) = 0, f'_m(\infty) = 0, \tag{57}$$

$$\theta_m(\infty) = 0, \begin{cases} \theta_m(0) = 0 & \text{for PST Case,} \\ \theta'_m(0) = 0 & \text{for PHF Case} \end{cases} \tag{58}$$

and

$$\chi_m = \begin{cases} 0 & m \leq 1 \\ 1 & m > 1 \end{cases} \tag{59}$$

$$f(\eta) = f_0(\eta) + \sum_{m=1}^{+\infty} f_m(\eta) p^m, \tag{60}$$

$$\theta(\eta) = \theta_0(\eta) + \sum_{m=1}^{+\infty} \theta_m(\eta) p^m, \tag{61}$$

## RESULTS AND DISCUSSION

As proved by Liao (1992), as long as the series solutions (Equations 60 and 61) are convergent, they should converge to one of the solutions of Equations 17 and 31. Note that the Equations 60 and 61 contain auxiliary parameters  $\hbar_1$  and  $\hbar_2$  which are not yet defined. These parameters play an important role in the framework of HAM. In fact, these parameters control the rate of convergence and the convergence region of the series. Proper values for these auxiliary parameters can be found by plotting the so-called  $\hbar$ -curves. When the valid region of  $\hbar$  is a horizontal line segment then the solution is converged. Figure 2 shows the  $\hbar_1$ -curve and Figures 3 and 4 show typical  $\hbar_2$ -curves for both PST and PHF cases for a given set of parameters,  $k_1 = 0.2, Mn = 1, Pr = 1, \beta = 0, \varepsilon = 0, r = 2, Nr = 0$

A wide valid zone is evident in these figures ensuring convergence of the series for both PST and PHF cases. Having chosen the best values for  $\hbar$ , we are able to present the velocity profiles obtained for different combinations of  $k_1$  and  $Mn$ , and investigate the effects of different parameters such as visco-elastic parameter,

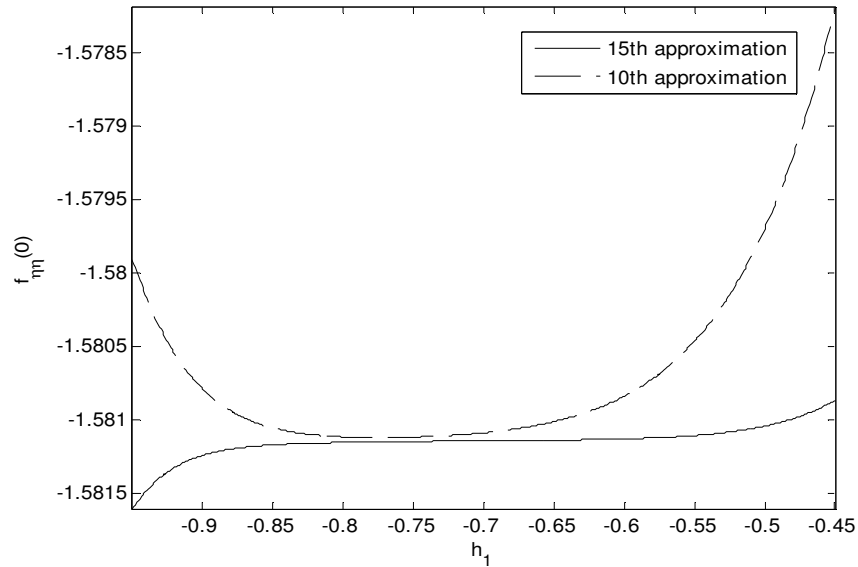


Figure 2. Typical  $\hat{h}_1$  -curve for  $k_1 = 0.2$ ,  $Mn = 1$ .

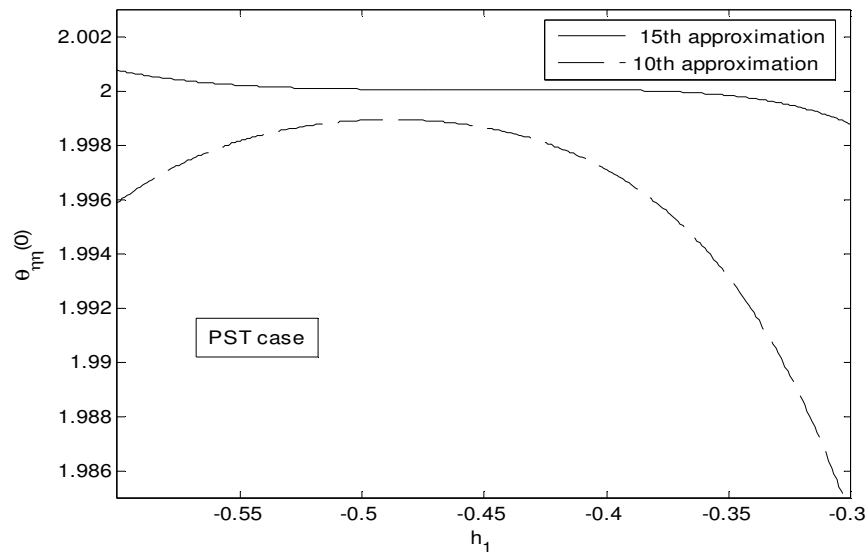
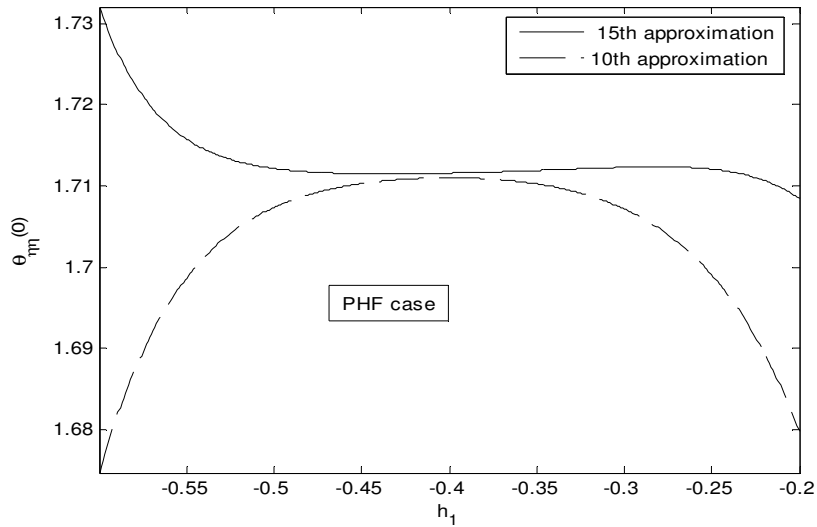


Figure 3. Typical  $\hat{h}_2$  -curves for  $k_1 = 0.2$ ,  $Mn = 1$ ,  $Pr = 1$ ,  $\beta = 0$ ,  $\epsilon = 0$ ,  $r = 2$ ,  $Nr = 0$ ,  $h_1 = -0.71$  for PST case.

radiation parameter, magnetic number, Prandtl number, wall temperature parameter, and heat source/sink parameter on the temperature field above the sheet for both PST and PHF cases. The obtained analytical results are illustrated in Figures 5 to 19 and Tables 1 and 2. Figure 5 is a graphical representation which depicts the effect of magnetic field parameter  $Mn$  on the horizontal velocity profile  $f''_\eta(\eta)$ . It is found that the effect of

magnetic field parameter  $Mn$  is to reduce the horizontal velocity profile  $f''_\eta(\eta)$ . This graphical representation reveals that magnetic field parameter  $Mn$  decreases the horizontal velocity profile  $f''_\eta(\eta)$ , significantly in the visco-elastic flow in comparison with the viscous flow, this is due to the fact that increase of  $Mn$  signifies the increase of Lorentz force, which opposes the horizontal



**Figure 4.** Typical  $\hat{h}_2$ -curves for  $k_1 = 0.2$ ,  $Mn = 1$ ,  $Pr = 1$ ,  $\beta = 0$ ,  $\varepsilon = 0$ ,  $r = 2$ ,  $Nr = 0$ ,  $h_1 = -0.71$  for PHF case.

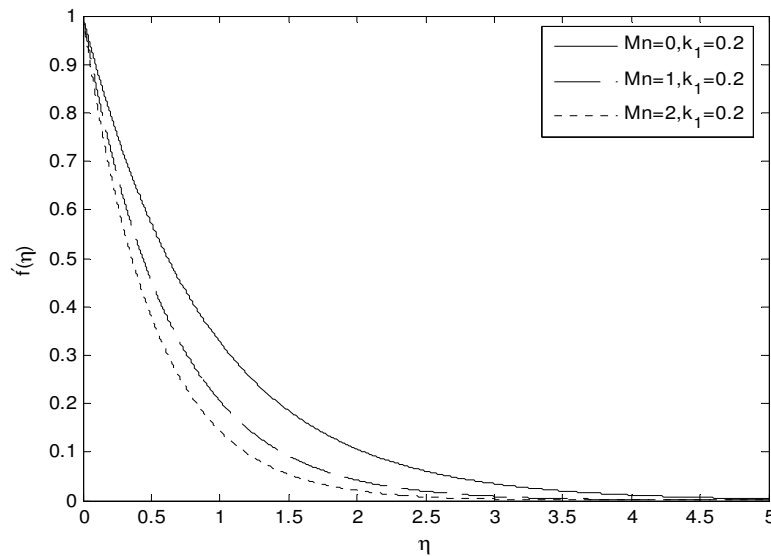


**Figure 5.** Effect of magnetic parameter  $Mn$  on horizontal velocity.

flow in the reverse direction. Figure 6 shows the effect of visco-elastic parameter,  $k_1$  on the horizontal velocity profile  $f_\eta(\eta)$ . The effect of visco-elastic parameter  $k_1$  is seen to decrease the boundary layer velocity throughout the boundary layer but significantly near the stretching sheet. Figures 7 and 8 represent variations in the transverse velocity for different numerical values of visco-elastic parameter  $k_1$  and magnetic parameter  $Mn$ . Obviously transverse velocity  $v$  is enhanced as visco-

elastic parameter  $k_1$  or magnetic parameter  $Mn$  rises. Idrees and Abel (1996) have shown that visco-elasticity acts physically to increase the adherence to the wall of the hydrodynamic boundary layer, which in turn retards the flow in the horizontal direction explaining the monotonically decreasing nature of the curves. The drag force appears as a term  $M_n f'$  in the transform momentum of Equation 17 and serves to retire the momentum in the positive direction of the  $x$ -axis, also affecting via the coupling with the other terms, the momentum in the

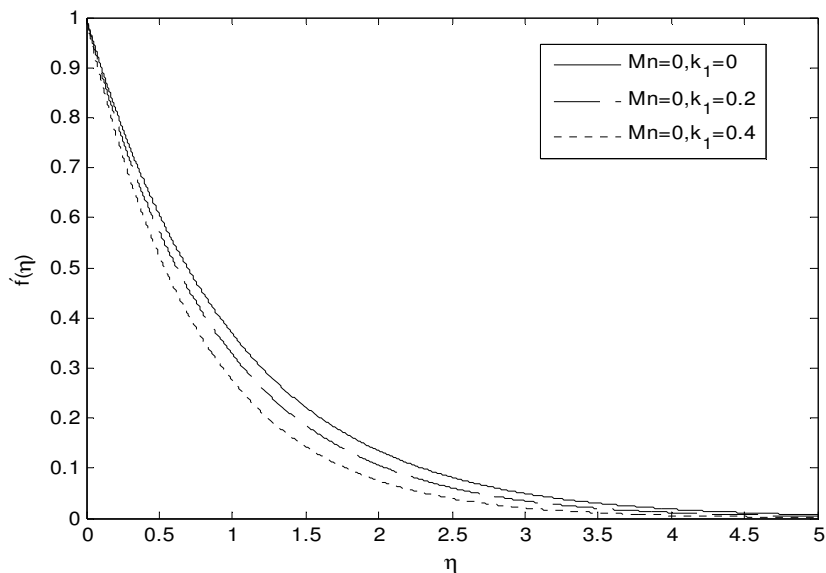


**Figure 6.** Effect of visco-elastic parameter  $k_1$  on horizontal velocity.

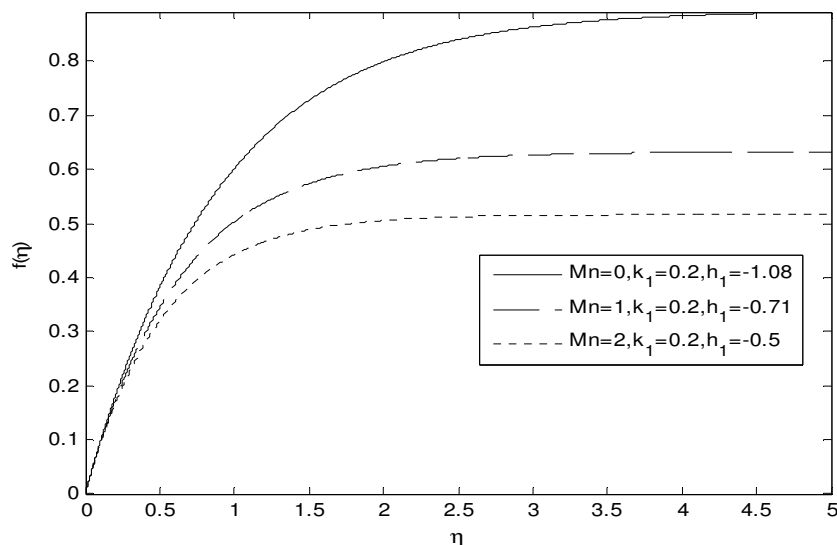


**Figure 7.** Effect of magnetic parameter  $Mn$  on transverse velocity.

the  $y$ -direction. The shear stresses are therefore lowered at the wall as  $Mn$  is increased, which decreases both  $u$  and  $v$  velocities. In both cases the maximum values of shear stress are reported at  $\eta = 0$ . These findings of the study correlate very well with the general conclusions arrived at by other classical magnetohydrodynamic studies including those of (Cramer and Pai, 1973; Siddheshwar and Mahabaleshwar, 2005). It is noted that the depression in the horizontal velocity is less prominent than the transverse velocity. Thus the influence of magnetic field is to aid more strongly in decelerating the

flow perpendicular to the plate. Figures 9 and 10 demonstrate the effect of visco-elastic parameter  $k_1$  on the temperature profile  $\theta(\eta)$  in the boundary layer in PST and PHF cases, respectively. It is observed that the temperature profile decreases in the boundary layer with the increase of distance from the boundary. It is also noticed that the temperature distribution is unchanged at the wall with the change of physical parameters. However, it tends to zero in the free stream. The temperature increases with the increasing values of visco-elastic parameter  $k_1$  both in the case of PST and

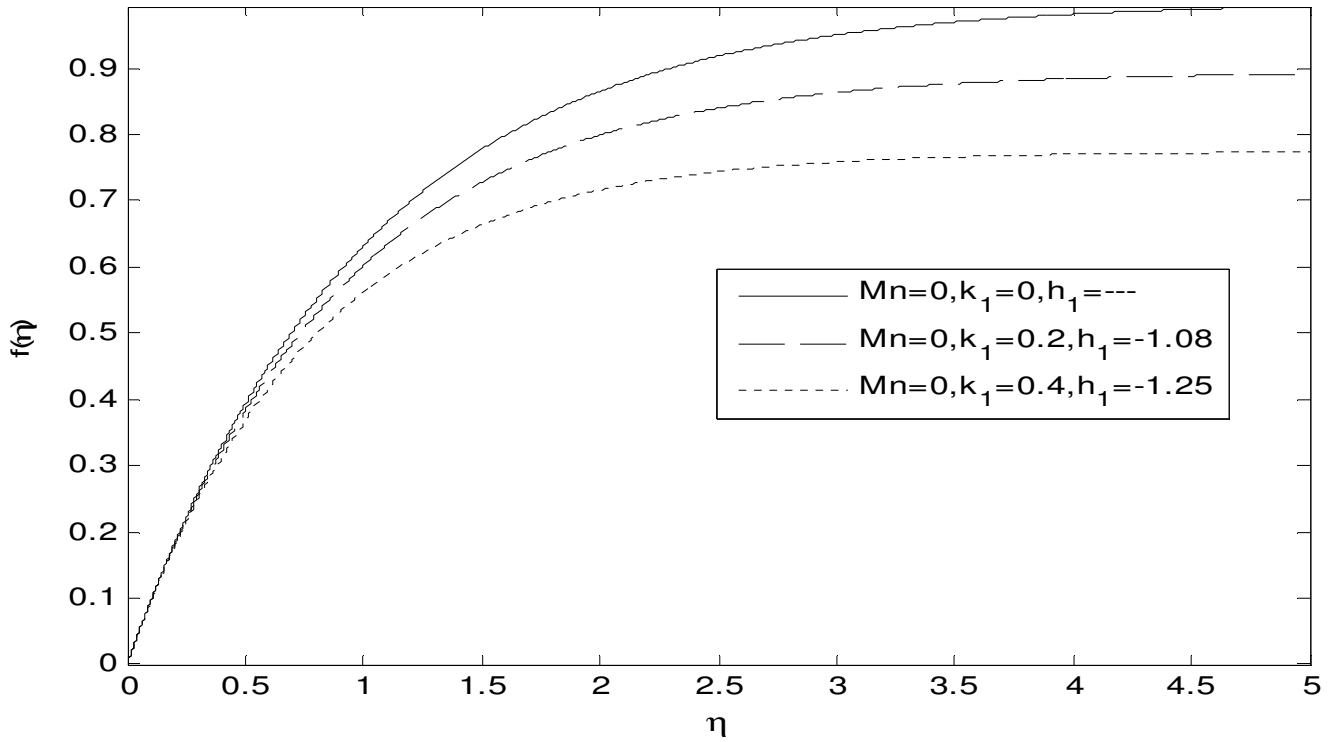


Figure 8. Effect of visco-elastic parameter  $k_1$  on transverse velocity.

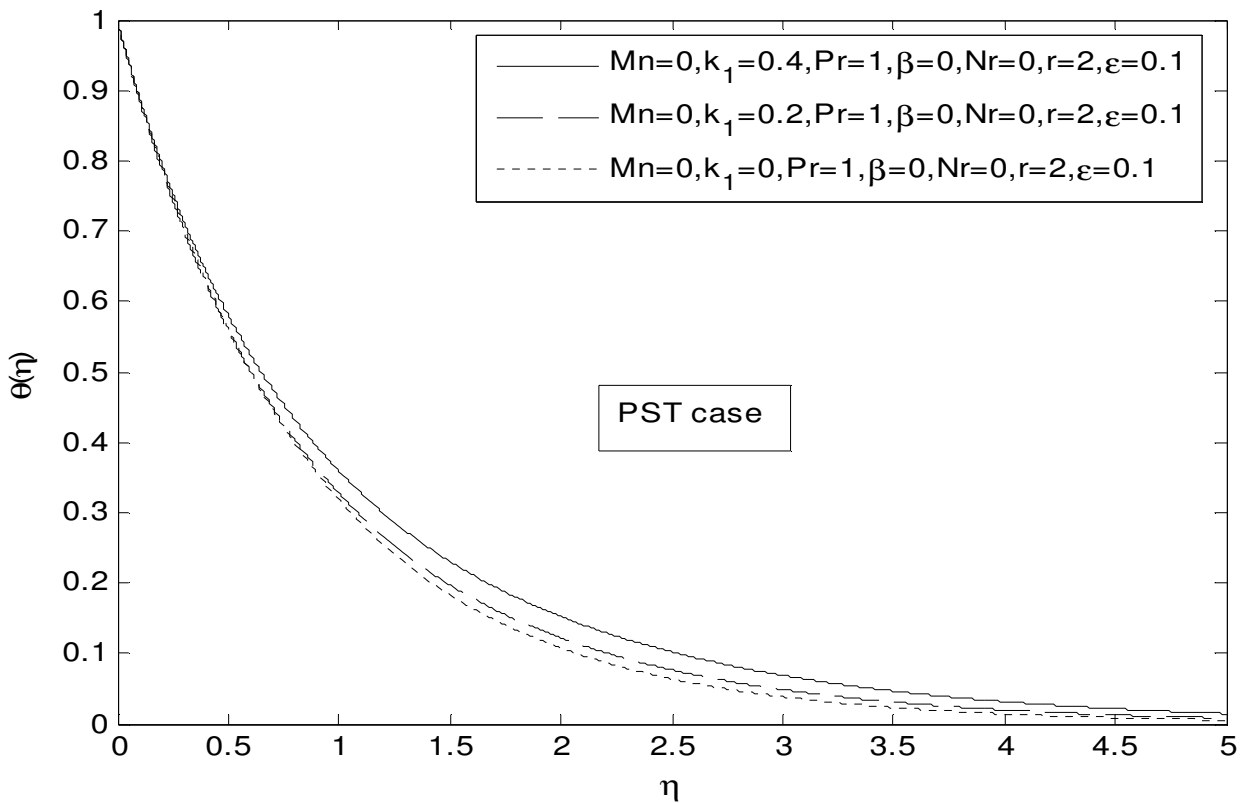


Figure 9. Effect of visco-elastic parameter  $k_1$  on the temperature profile in  $\theta(\eta)$  PHF case.

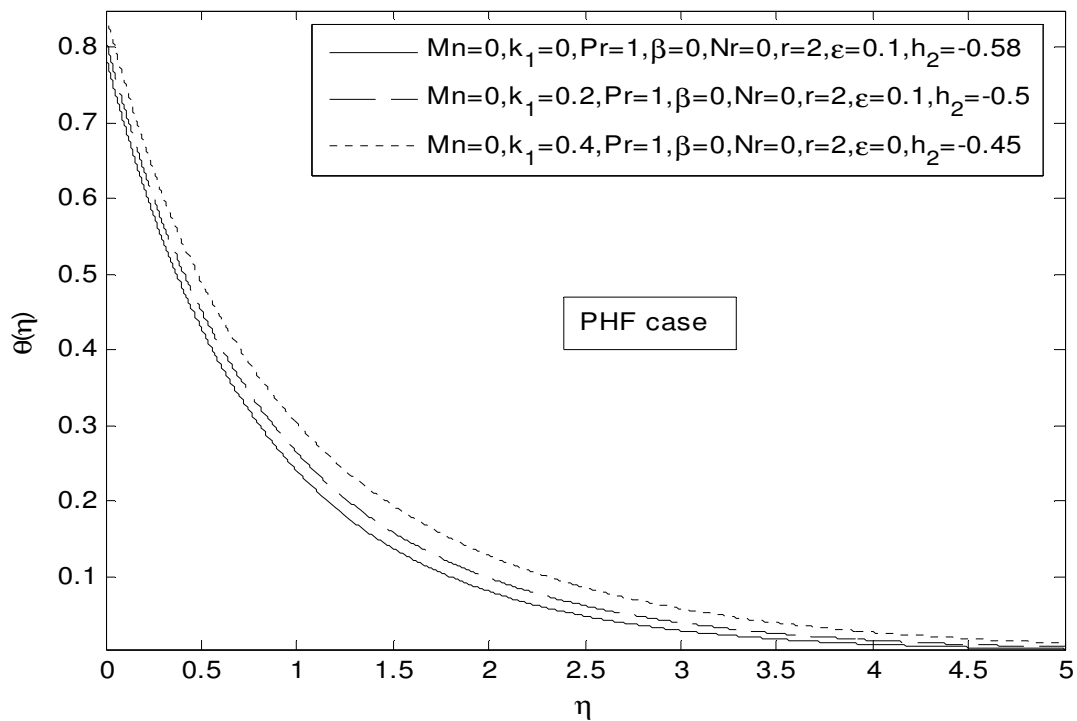


Figure 10. Effect of visco-elastic parameter  $k_1$  on the temperature profile in  $\theta(\eta)$  PHF case.

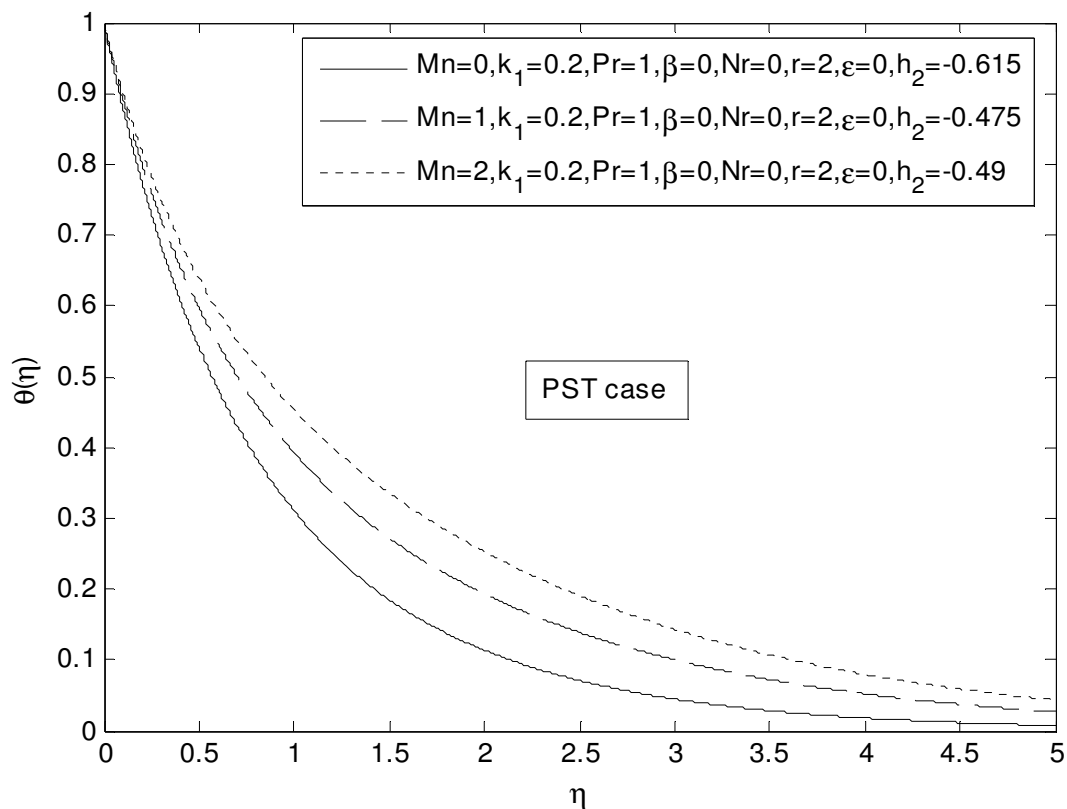


Figure 11. Effect of magnetic parameter  $Mn$  on temperature profile in  $\theta(\eta)$  PST case.

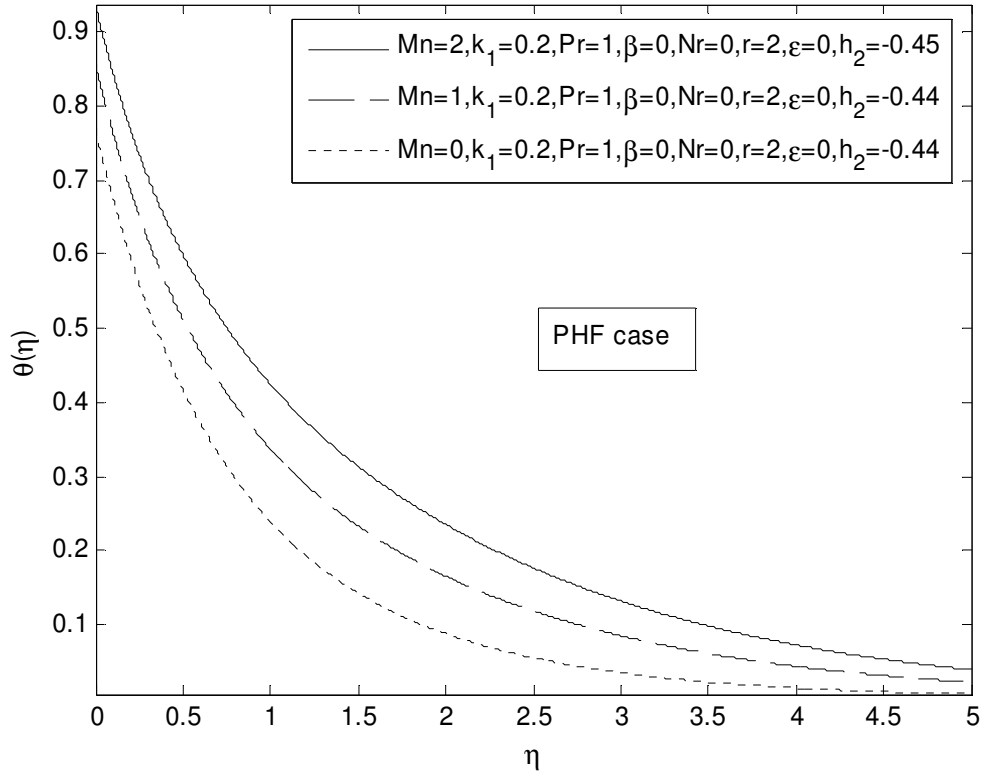


Figure 12. Effect of magnetic parameter  $Mn$  on temperature profile  $\theta(\eta)$  in PHF case.

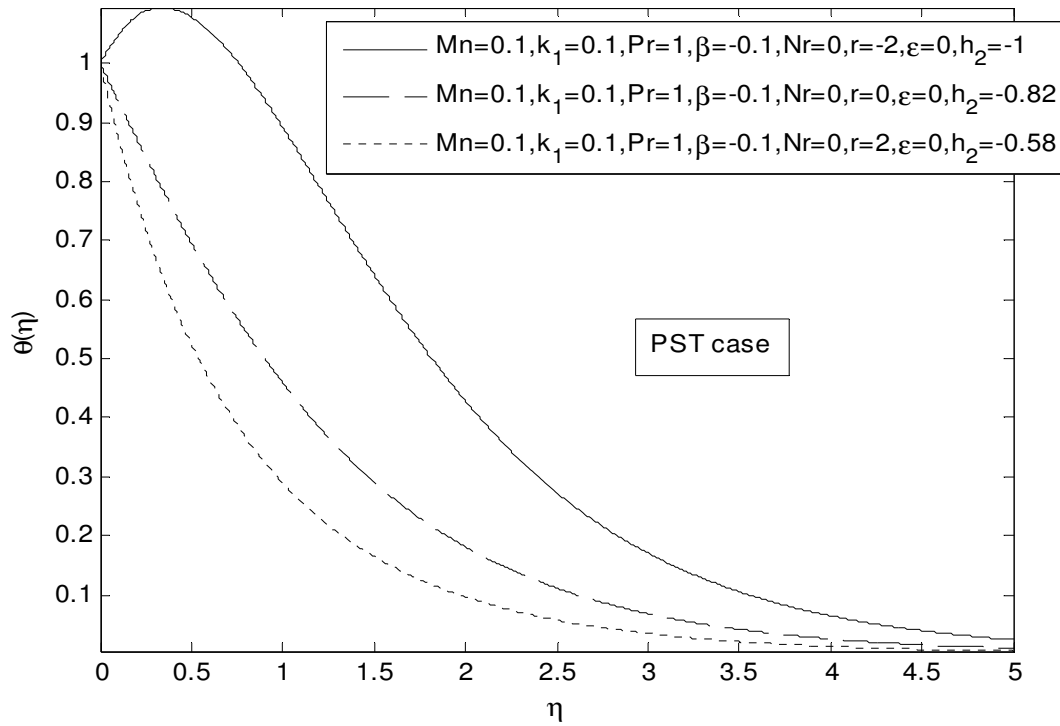
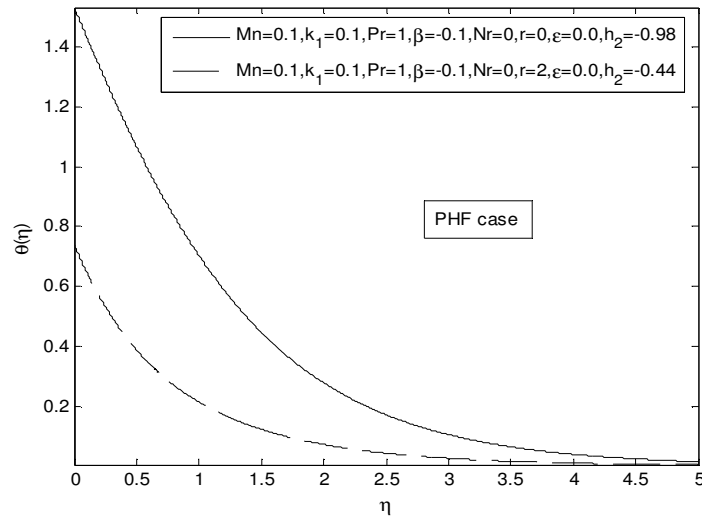


Figure 13. Effect of wall temperature parameter  $r$ , on the temperature profile  $\theta(\eta)$  in PST case.



**Figure 14.** Effect of wall temperature parameter  $r$ , on the temperature profile  $\theta(\eta)$  in PHF case.

PHF. This is due to the fact that the thickening of thermal boundary layer occurs due to the increase of visco-elastic normal stress. From Tables 1 and 2, we observe that the effect of visco-elastic parameter is to increase the wall temperature gradient  $-\theta_{\eta}(0)$  in PST case and the wall temperature  $\theta(0)$  in PHF case. The effect of magnetic parameter  $Mn$  on temperature profile  $\theta(\eta)$  in the presence/absence of variable thermal conductivity is shown in Figures 11 and 12 in case of PST and PHF, respectively. It is noticed that the effect of magnetic parameter is to increase the temperature profile  $\theta(\eta)$  in the boundary layer. This is because of the fact that the introduction of transverse magnetic field to an electrically conducting fluid gives rise to a body force known as Lorentz force which opposes the motion. The resistance offered to the flow because of this force is responsible in enhancing the temperature. Also, the effect on the flow and thermal fields become more so as the strength of the magnetic field increases. The effect of magnetic parameter  $Mn$  is to increase the wall temperature gradient  $-\theta_{\eta}(0)$  in PST case and the wall temperature  $\theta(0)$  in PHF case. This is due to the fact that thermal boundary layer thickness decreases as the magnetic parameter  $Mn$  increases which results in higher temperature gradient at the wall and hence higher heat transfer at the wall. For fixed values of Prandtl number and magnetic parameter the effect of wall temperature parameter  $r$ , on the temperature profile  $\theta(\eta)$  in the boundary layer is shown in Figures 13 and 14. From the graphical representation we observe that the increase in wall temperature parameter  $r$  leads the temperature

profile  $\theta(\eta)$  to decrease and the magnitude of wall temperature gradient increases with wall temperature. This is due to the fact that, when  $r > 0$ , heat flows from the stretching sheet into the ambient medium and, when  $r < 0$ , the temperature gradient is positive and heat flows into the stretching sheet from the ambient medium. Figures 15 and 16 shows the effect of thermal radiation on temperature profile  $\theta(\eta)$  in the boundary layer. It is observed that the increase in thermal radiation parameter  $Nr$  produces a significant increase in the thickness of the thermal boundary layer of the fluid and so the temperature profiles  $\theta(\eta)$  increases. The wall gradients of PST and PHF cases increase as the thermal radiation parameter increases which can be observed in Tables 1 and 2. The effect of heat source/sink parameter  $\beta$  on temperature profile  $\theta(\eta)$  in the boundary layer is shown in Figures 17 and 18. It is observed that the effect of heat source  $\beta > 0$  in the boundary layer generates the energy which causes the temperature to increase, while the presence of heat sink  $\beta < 0$  in the boundary layer absorbs the energy which causes the temperature to decrease. From Tables 1 and 2 we see that the effect of heat source is more pronounced as compared to that of heat sink. These behaviours are even true in the presence of variable thermal conductivity. Figures 19 and 20 demonstrate the effect of Prandtl number on temperature profile in the boundary layer. It is seen that the effect of Prandtl number is to decrease the temperature profile in the boundary layer. This is because of the fact that thermal boundary thickness decreases with increase in Prandtl number. It is also observed from

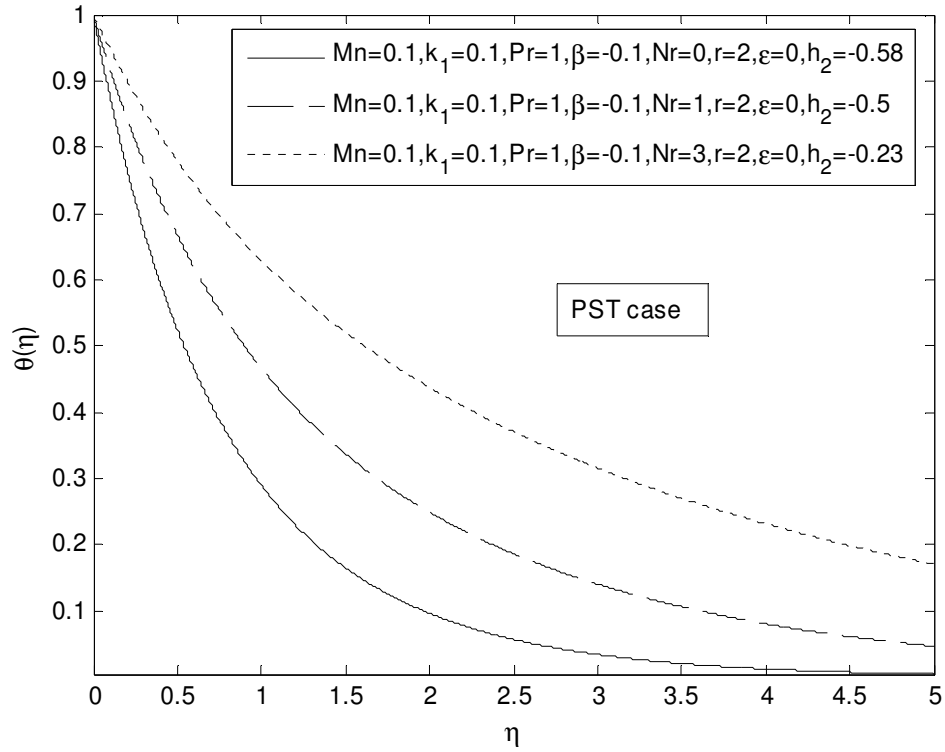


Figure 15. Effect of thermal radiation on temperature profile  $\theta(\eta)$  in PST case.

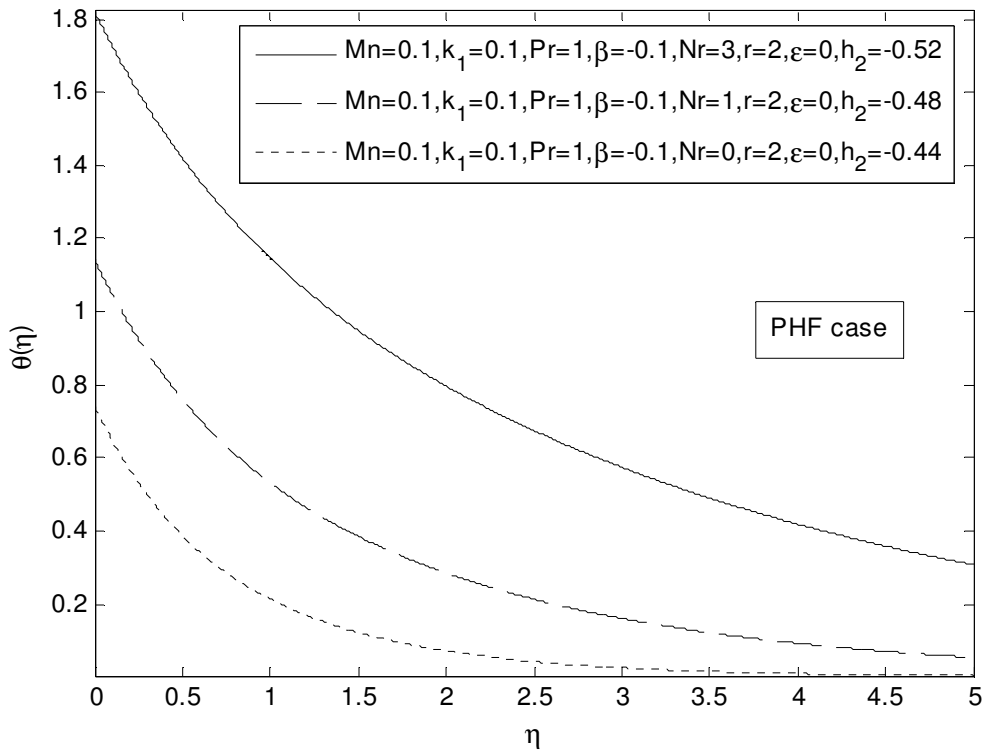
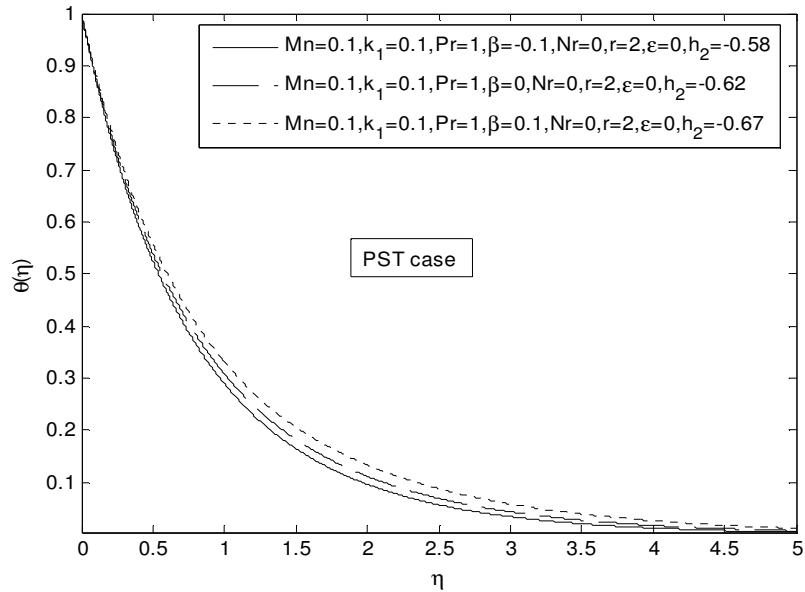
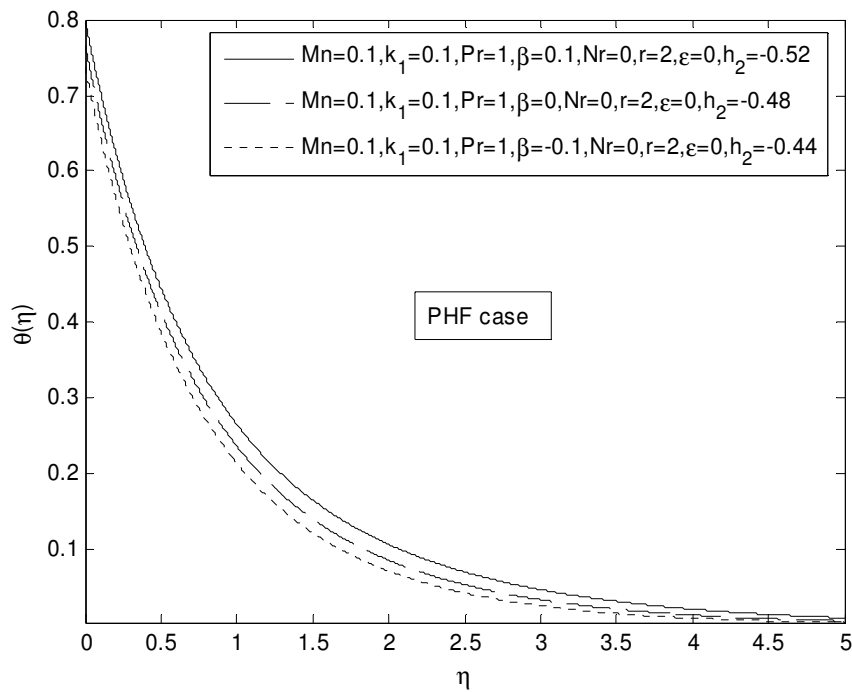


Figure 16. Effect of thermal radiation on temperature profile  $\theta(\eta)$  in PHF case.



**Figure 17.** Effect of heat source/sink parameter  $\beta$  on temperature profile in PST case.



**Figure 18.** Effect of heat source/sink parameter  $\beta$  on temperature profile in PST case.

Tables 1 and 2 that the heat transfer increases with Prandtl number because a higher Prandtl number fluid has relatively lower thermal conductivity which reduces conduction and there by increases the variation. This results in the reduction of the thermal boundary layer

thickness and increase in the heat transfer at the wall. For PHF case, the temperature at the wall reduces as the Prandtl number increases because of the cooling effect on the surface caused by the increase in Prandtl number. Many other analytical methods investigated in many

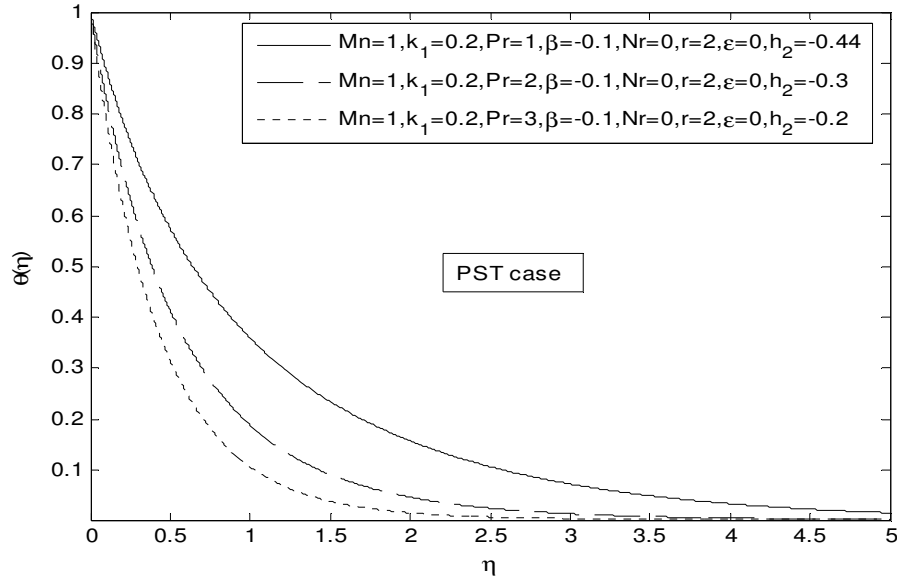


Figure 19. Effect of Prandtl number on temperature profile in PST case.

Table 1. The best values of the auxiliary parameters and Wall temperature gradients  $\theta_\eta(0)$  for the PST case.

$k_1$	Pr	$\beta$	$\epsilon$	$r$	$Nr$	$Mn$	$\hbar_1$	$\hbar_2$	$\theta_\eta(0)$
0	1	0	0	2	0	1	-0.69	-0.47	-1.2155
0.2	1	0	0	2	0	1	-0.71	-0.44	-1.16859
0.4	1	0	0	2	0	1	-0.72	-0.53	-1.10125
0.1	1	-0.1	0	2	0	0.1	-0.98	-0.58	-1.35219
0.1	1	0	0	2	0	0.1	-0.98	-0.62	-1.30354
0.1	1	0.1	0	2	0	0.1	-0.98	-0.67	-1.24954
0.1	1	-0.1	0	2	1	0.1	-0.98	-0.5	-0.87594
0.1	1	-0.1	0	2	3	0.1	-0.98	-0.23	-0.54886
0.1	1	-1	0	0	0	0.1	-0.98	-0.82	-0.65243
0.1	1	-1	0	-2	0	0.1	-0.98	-1	-0.58039
0.2	1	0	0	2	0	0	-1.08	-0.64	-1.3
0.2	1	0	0	2	0	2	-0.5	-0.51	-1.07009
0.2	1	-0.1	0	2	0	1	-0.71	-0.44	-1.23432
0.2	2	-0.1	0	2	0	1	-0.71	-0.3	-1.896
0.2	3	-0.1	0	2	0	1	-0.71	-0.2	-2.2922

scientific papers (Bayat et al., 2010, 2011a, b, c, d, e, f, g; Pakar et al., 2011; Shahidi et al., 2011; Soleimani Kutanaei, 2011; ganji et al., 2009; Hosein Nia et al., 2009).

**CONCLUSION**

In this study the homotopy analysis method (HAM) was successfully applied on steady MHD flow and heat

transfer in a visco-elastic fluid flow over a semi-infinite, impermeable, non-isothermal stretching sheet with internal heat generation/absorption in the presence of radiation. The accuracy of the method was investigated by a comparison which was made between numerical ones. The excellent agreement of the HAM solutions and the numerical ones show the reliability and the efficiency of the method. The homotopy analysis method (HAM) provides efficient alternative tools in solving non-linear equations. The method is useful to obtain analytical

**Table 2.** The best values of the auxiliary parameters and wall temperature  $\theta(0)$  for the PHF case.

$k_1$	Pr	$\beta$	$\epsilon$	$r$	$Nr$	$Mn$	$\tilde{h}_1$	$\tilde{h}_2$	$\theta(0)$
0	1	-0.1	0	2	0	1	-0.69	-0.4	0.78601
0.2	1	-0.1	0	2	0	1	-0.71	-0.37	0.81025
0.4	1	-0.1	0	2	0	1	-0.72	-0.46	0.97915
0.1	1	-0.1	0	2	0	0.1	-0.98	-0.44	0.73953
0.1	1	0	0	2	0	0.1	-0.98	-0.48	0.76712
0.1	1	0.1	0	2	0	0.1	-0.98	-0.52	0.80024
0.1	1	-0.1	0	2	1	0.1	-0.98	-0.48	1.14161
0.1	1	-0.1	0	2	3	0.1	-0.98	-0.3	1.82175
0.1	1	-0.1	0	0	0	0.1	-0.98	-0.98	1.53271
0.2	1	-0.1	0	2	0	0	-1.08	-0.42	0.74127
0.2	1	-0.1	0	2	0	2	-0.5	-0.41	0.87655
0.2	1	-0.1	0	2	0	1	-0.71	-0.37	0.81025
0.2	2	-0.1	0	2	0	1	-0.71	-0.19	0.52466
0.2	3	-0.1	0	2	0	1	-0.71	-0.13	0.42053

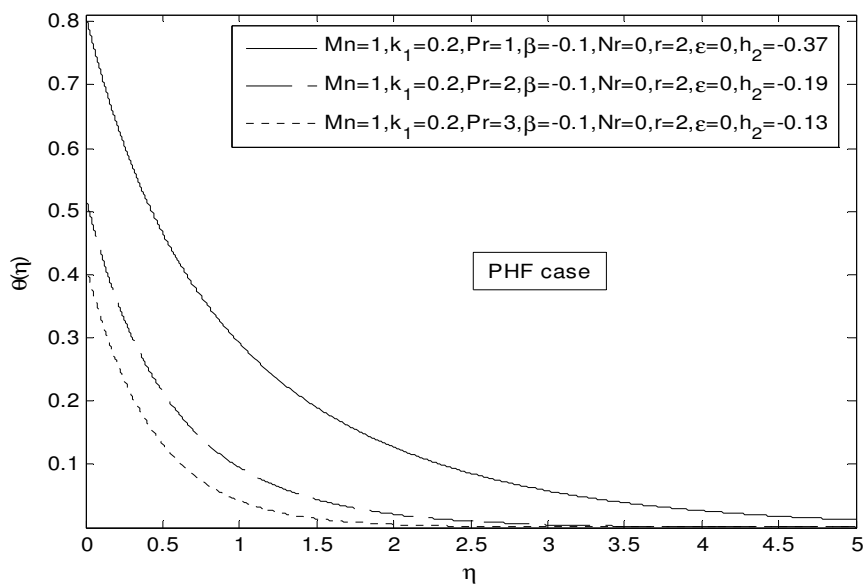


**Figure 20.** Effect of Prandtl number on temperature profile in PHF case.

solution for all non-linear equations.

**REFERENCES**

Abel MS, Veena PH (1998). Visco-elastic fluid flow and heat transfer in a porous medium over a stretching sheet. *Int. J. non-Linear Mech.*, 33: 531–8.  
 Andersson HI (1992). MHD flow of a visco-elastic fluid past a stretching surface. *Acta Mech.*, 95:227–30.  
 Bujurke NM, Biradar SN, Hiremath PS (1987). Second order fluid flow past a stretching sheet with heat transfer. *Angew Math. Phys.*, (ZAMP), 38:653–7.  
 Beard DW, Walters K (1964). Elastic–viscous boundary layer flows,

two-dimensional flow near a stagnation point. *Proc. Cambr. Phil. Soc.*, 60: 667–74.  
 Bararnia H, Ghasemi E, Domairry G, Soleimani S(2010). Behavior of micro-polar flow due to linear stretching of porous sheet with injection and suction, *Adv. Eng. Softw.*, 41: 893–897.  
 Bayat M, Shahidi M, Barari A, Domairry G (2010). The Approximate Analysis of Nonlinear Behavior of Structure under Harmonic Loading, *Int. J. Phy. Sci.*, 5(7):1074-1080.  
 Bayat M, Shahidi M, Barari A, Domairry G (2011a). Analytical Evaluation of the Nonlinear Vibration of Coupled Oscillator Systems. *Zeitschrift fur Naturforschung Section A-A J. Phys. Sci.*, 66(1-2): 67-74.  
 Bayat M, Barari A, Shahidi M (2011b). Dynamic Response of Axially Loaded Euler-Bernoulli Beams, *Mechanika*, 17(2): 172-177.  
 Bayat M, Bayat M, Bayat M (2011c). An Analytical Approach on a Mass

- Grounded by Linear and Nonlinear Springs in Series, *Int. J. Phy. Sci.*, 6(2): 229–236.
- Bayat M, Shahidi M, Bayat M (2011d). Application of Iteration Perturbation Method for Nonlinear Oscillators with Discontinuities, *Int. J. Phy. Sci.*, 6(15): 3608-3612.
- Bayat M, Pakar I, Bayat M (2011e). Analytical Study on the Vibration Frequencies of Tapered Beams, *Latin Am. J. Solids Struct.*, 8(2): 149–162.
- Bayat M, Abdollahzadeh G (2011f). Analysis of the steel braced frames equipped with ADAS devices under the far field records, *Latin Am. J. Solids Struct.*, 8(2): 163 – 181.
- Bayat M, Pakar I (2011g). Application of He's Energy Balance Method for Nonlinear vibration of thin circular sector cylinder, *Int. J. Phy. Sci.*, In press.
- Crane LJ (1970). Flow past a stretching plate. *Z Angew Math. Phys.*, 21:645–7.
- Chen CK, Char MI (1988). Heat transfer of a continuous stretching surface with suction or blowing. *J. Math. Anal. Appl.*, 1988; 135:568–80.
- Chiam TC (1977). Magneto-hydrodynamic heat transfer over a non-isothermal stretching sheet. *Acta Mech.*, 122:169–79.
- Chiam TC (1996). Heat transfer with variable thermal conductivity in a stagnation point towards a stretching sheet. *Int. Comm. Heat Mass Transfer*, 23(2):239–48.
- Chiam TC (1988). Heat transfer in a fluid with variable thermal conductivity over a linearly stretching sheet. *Acta Mech.*, 129:63–72.
- Chakrabarti A, Gupta AS (1979). Hydro-magnetic flow and heat transfer over a stretching sheet. *Quart. Appl. Math.*, 37:73–8.
- Char MI (1994). Heat and mass transfer in a hydro-magnetic flow of a visco-elastic fluid over a stretching sheet. *J. Math. Anal. Appl.*, 186:674–89.
- Cramer KR, Pai SI (1973), *Magneto-fluid Dynamics for Engineers and Applied, Physicists*, McGraw-Hill, New York.
- Datti PS, Prasad KV, Subhas Abel M, Ambuja Joshi (2004). MHD fluid flow over a nonisothermal stretching sheet. *Int. J. Eng. Sci.*, 42:935–46.
- Datta BK, Roy P, Gupta AS (1985). Temperature field in the flow over a stretching sheet with uniform heat flux. *Int. Comm. Heat Mass Transfer*, 12:89–94.
- Ganji DD, Rafei M, Sadighi A, Ganji ZZ(2009), A Comparative Comparison of He's Method with Perturbation and Numerical Methods for Nonlinear Vibrations Equations, *Int. J. Nonlinear Dyn. Eng. Sci.*, 1 (1); 1-20.
- Gupta PS, Gupta AS (1977). Heat and mass transfer on a stretching sheet with suction or blowing. *Can. J. Chem. Eng.*, 55:744–6.
- Hosein NSH, Ranjbar A, Soltani H, Ghasemi J (2009), Effect of the Initial Approximation on Stability and Convergence in Homotopy Perturbation Method, *Int. J. Nonlinear Dyn. Eng. Sci.*, 1(1):79-98.
- Rajagopal KR, Na TY, Gupta AS (1984). Flow of a visco-elastic fluid over a stretching sheet. *Rheol. Acta.*, 23:213–5.
- Liao SJ (1992). The proposed homotopy analysis techniques for the solution of nonlinear problems. PhD dissertation. Shanghai: Shanghai Jiao Tong University [in English].
- Liao SJ (1992). A second-order approximate analytical solution of a simple pendulum by the process analysis method. *J. Appl. Mech. Trans., ASME*, 59:970.
- Liao SJ (1997). A kind of approximate solution technique which does not depend upon small parameters (II): an application in fluid mechanics. *Int. J. Non-linear Mech.*, 32:815.
- Liao SJ (1999). An explicit totally analytic approximation of Blasius viscous flow problems. *Int. J. Non-linear Mech.*, 34:759.
- Liao SJ (2003). *Beyond perturbation: introduction to homotopy analysis method*. Boca Raton: Chapman & Hall/CRC Press.
- Liao SJ (1999). A uniformly valid analytic solution of two-dimensional viscous flow over a semi-infinite flat plate. *J. Fluid Mech.*, 385:101.
- Liao SJ (2002), Campo A. Analytic solutions of the temperature distribution in Blasius viscous flow problems. *J. Fluid Mech.*, 453:411.
- Liao SJ (2003). On the analytic solution of magnetohydrodynamic flows of non-Newtonian fluids over a stretching sheet. *J. Fluid Mech.*, 488:189.
- McLeod B, Rajagopal KR (1987). On the non-uniqueness of the flow of a Navier-Stokes fluid due to stretching boundary. *Arch. Ration Mech. Anal.*, 98:385–493.
- Idrees MK, Abel MS (1996). Visco-elastic flow past a stretching sheet in porous media and heat transfer with internal heat source, *Indian J. Theor. Phys.*, 44:233–244.
- Liao SJ, Tan Y (2007). A general approach to obtain series solutions of nonlinear differential equations. *Stud. Appl. Math.*, pp. 119:297.
- Prasad KV, Subhas Abel, Khan SK (2000). Momentum and heat transfer in a visco-elastic fluid flow in a porous medium over a non-isothermal stretching sheet. *Int. J. Numer. Meth. Heat Fluid Flow*, 10(8):786–801.
- Prasad KV, Subhas AM, Datti PS (2003). Diffusion of chemically reactive species of a non-Newtonian fluid immersed in a porous medium over a stretching sheet. *Int. J. Non-Linear Mech.*, 38(5):651–7.
- Pavlov KB (1974). Magneto-hydrodynamic flow of an incompressible viscous fluid caused by deformation of a plane surface. *Magninaya Gidrodinamika (USSR)*, 4:146–7.
- Pakar I, Bayat M (2011). Application of the Energy Balance Method for high nonlinear single degree of freedom, *Int. J. Phy. Sci.*, (In press).
- Quinn BM (1992), *Thermal radiative transfer properties*, John Wiley and Sons, New York.
- Moghim SM, Domairry G, Soheil S, Ghasemi E, Bararnia H (2010). Application of homotopy analysis method to solve MHD Jeffery–Hamel flows in non-parallel walls, doi:10.1016/j.advengsoft.2010.12.007.
- Siddappa B, Abel MS (1985). Non-Newtonian flow past a stretching plate. *Z. Angew. Math. Phys.*, 36:47–54.
- Sam LP, Nageswara RB (1995). The non-uniqueness of the MHD flow of a viscoelastic fluid past a stretching sheet. *Acta Mech.*, 112:223–5.
- Shahidi M, Bayat M, Pakar I, Abdollahzadeh GR (2011). On the solution of free non-linear vibration of beams, *Int. J. Phy. Sci.*, 6(7): 1628–1634, 2011.
- Sarpakaya T (1961). Flow on non-Newtonian fluids in a magnetic field. *Am. Inst. Chem. Ing. J.*, 7:26–8.
- Siddheshwar PG, Mahabaleshwar US (2005), Effects of radiation and heat source on MHD flow of a visco-elastic liquid and heat transfer over a stretching sheet, *Int. J. Non-Linear Mech.*, 40 :807–821.
- Soleimani KS, Ghasemi E, Bayat M (2011). Mesh-free Modeling of Two-Dimensional Heat Conduction Between Eccentric Circular Cylinders, *Int. J. Phy. Sci.*, 6(16):4044-4052.
- Troy WC, Overmann II EA, Eremont-Rout GB, Keener JP (1987). Uniqueness of the flow of second order fluid flow past a stretching sheet. *Quart. Appl. Math.*, 44:753–5.
- Wen-Dong C (1989). The non-Uniqueness of the flow of a visco-elastic fluid over a stretching sheet. *Quart. Appl. Math.*, 47:365–6.
- Xu H, Liao SJ (2005). Series solutions of unsteady magnetohydrodynamic flows of non-Newtonian fluids caused by an impulsively stretching plate. *J. Non-Newton Fluid Mech.*, 159:46.